

Article

Identifying Graphite Purity by Weighted Fusion Method

Xiaoping Xu ¹, Xiangjia Yu ¹, Guangjun Liu ^{1,*} and Feng Wang ²

¹ School of Sciences, Xi'an University of Technology, Xi'an 710054, China; xpxuxaut@sina.com (X.X.); xjyuxaut@sina.com (X.Y.)

² School of Mathematics and Statistics, Xi'an Jiaotong University, Xi'an 710049, China; wangf@xjtu.edu.cn

* Correspondence: chenliu@xaut.edu.cn

Abstract: The purity of graphite often affects its application in different fields. In view of the low efficiency of manual recognition and the omission of features extracted by single convolution neural network, this paper proposes a method for identifying graphite purity using a multi-model weighted fusion mechanism. The ideas suggested in this paper are as follows. On the self-built small sample data set, offline expansion and online enhancement are carried out to improve the generalization ability of the model and reduce the overfitting problem of deep convolution neural networks. Combined with transfer learning, a dual-channel convolution neural network is constructed using the optimized Alex Krizhevsky Net (AlexNet) and Alex Krizhevsky Net 50 (AlexNet50) to extract the deep features of the graphite image. After the weighted fusion of the two features, the Softmax classifier is used for classification. Experimental results show that recognition accuracy after weighted fusion is better than that of single network, reaching 97.94%. At the same time, the stability of the model is enhanced, and convergence speed is accelerated, which proves the feasibility and effectiveness of the proposed method.

Keywords: graphite; purity; fusion; convolution neural network; transfer learning



Citation: Xu, X.; Yu, X.; Liu, G.;

Wang, F. Identifying Graphite Purity by Weighted Fusion Method.

Processes **2022**, *10*, 416. <https://doi.org/10.3390/pr10020416>

Academic Editor: Jacopo Donnini

Received: 3 December 2021

Accepted: 15 February 2022

Published: 21 February 2022

Publisher's Note: MDPI stays neutral with regard to jurisdictional claims in published maps and institutional affiliations.



Copyright: © 2022 by the authors. Licensee MDPI, Basel, Switzerland. This article is an open access article distributed under the terms and conditions of the Creative Commons Attribution (CC BY) license (<https://creativecommons.org/licenses/by/4.0/>).

1. Introduction

In the development of high-tech industry, graphite plays an increasingly important role. The world has gradually entered the carbon era from the silicon era. Graphite's unique physical characteristics enable it to be applied in various fields of the national economy and people's livelihoods, with very important industrial value [1–4]. Many developed countries have listed graphite as a key mineral and have implemented a series of strategic plans.

At present, with the continuous expansion of the application field of graphite, its purity required to become higher and higher. Graphite itself is a natural elemental crystalline mineral of carbon, and the fixed carbon content is the main index of graphite purity [5]. According to the fixed carbon content, it can be divided into four categories: high-purity graphite ($\omega(C) \geq 99.9\%$); high-carbon graphite ($94.0\% \leq \omega(C) < 99.9\%$); medium-carbon graphite ($80.0\% \leq \omega(C) < 94.0\%$); and low-carbon graphite ($50.0\% \leq \omega(C) < 80.0\%$). Graphite purity measurement detects the proportion of fixed carbon content in graphite. Graphite has good chemical stability at room temperature, so it is not convenient to directly determine its carbon content. Generally, high-temperature volatilization of materials to be tested is used to calculate the carbon content. This method has high time cost and low accuracy, due to the need for manual identification. With the increasing importance of image processing, analysis and application in the mining field, the deep convolution neural networks (CNN) structure is used in many recognition applications to achieve high recognition accuracy [6]. CNN contains high-level semantic information and middle-level details, which can improve the accuracy of recognition. Therefore, the model proposed in this paper is based on CNN architecture. The samples with different purity of graphite have little difference, so it is necessary to train a deeper network layer to improve the accuracy of graphite recognition. However, the design of a deep network can produce a large number

of redundant parameters, even overfitting problems, while a shallow network with fewer parameters is not enough to learn the graphite's feature representation. Therefore, the combination of multiple features provides the possibility to solve this problem. Compared with a single feature type, the combination of multiple features has better performance [7]. At present, multi-model fusion is widely used in classification and recognition. Li et al. weighted the Local Binary Pattern (LBP) features and the features extracted from Visual Geometry Group 16 (VGG16) network, then fused the features to complete six kinds of expression classification [8]; Brahimi et al. solved the problem of tomato leaf disease recognition by using the existing CNN model pre-trained by AlexNet and Google LeNet (GoogLeNet) [9]. Although image recognition technology continues to develop and improve with the progress of science and technology, the relevant recognition of graphite still adopts physical and chemical methods such as manual recognition and microscope recognition. At present, there is little research on the image recognition of graphite purity. In particular, the difficulty of graphite data collection and the strong professionalism of graphite research also lead to the difficult development of intelligent recognition of graphite. Generally speaking, measuring the proportion of fixed carbon content in graphite can achieve the purpose of detecting its purity, but graphite has excellent chemical stability at room temperature. The steps of directly determining its carbon content are cumbersome and the requirements of the measurement environment are high. Based on this, at present, the purity measurement of graphite is mostly calculated by high-temperature volatilization, that is, according to the volatilization value when graphite is oxidized to carbon dioxide at high temperature. Although this method reduces the difficulty of measurement, it takes a long time and has low manual recognition accuracy. The convolution neural network based on migration learning enables rapid, efficient recognition of graphite purity. Therefore, the realization of automatic identification of graphite purity is of great significance to the development of the graphite field. Based on this, combined with transfer learning, this paper improves the classical CNN network to accelerate the convergence of the model, save time and cost, and realize the intelligent recognition of the graphite image.

In the multi-pool convolution operation, multi-layer features may lose the information of depth, shape and the relationship between the target and the scene, which limits recognition accuracy [10]. In the first mock exam, we extract the deep-level characteristics of graphite images based on the optimized AlexNet network and ResNet50 network design of the two-channel convolution network model. We assign weights to the features of the dual-channel CNN and obtain a higher recognition rate of than the single model [11].

The innovations of this paper are as follows: (1) using data augmentation (brightness enhancement, contrast enhancement, horizontal rotation and random direction rotation) to solve the problem of model classification for small sample data; (2) the feature of the image is extracted using the migration learning algorithm, which greatly shortens the training time of the model; (3) building the optimized model of double-channel weighted fusion network of AlexNet and ResNet50. The flowchart of the graphite purity identification algorithm is shown in Figure 1.

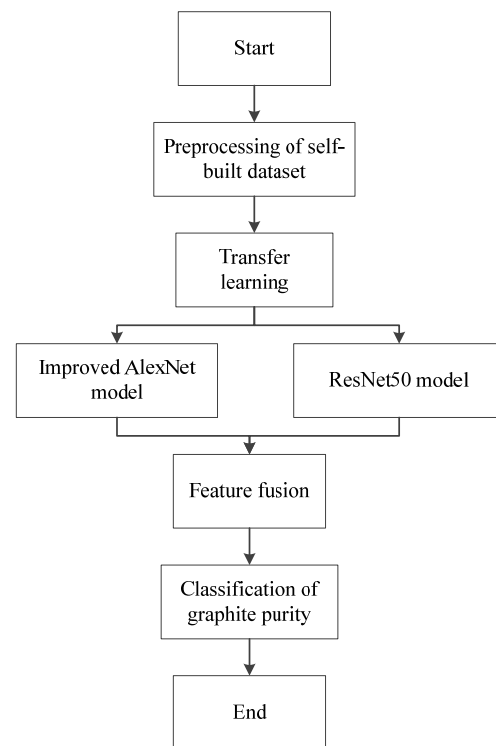


Figure 1. Overall framework of graphite purity identification algorithm.

2. Image Processing

2.1. Data Set Establishment

The data set of this paper is collected from the existing graphite in the laboratory, and the specific collection situation is shown in Figure 2 (carbon content in brackets).

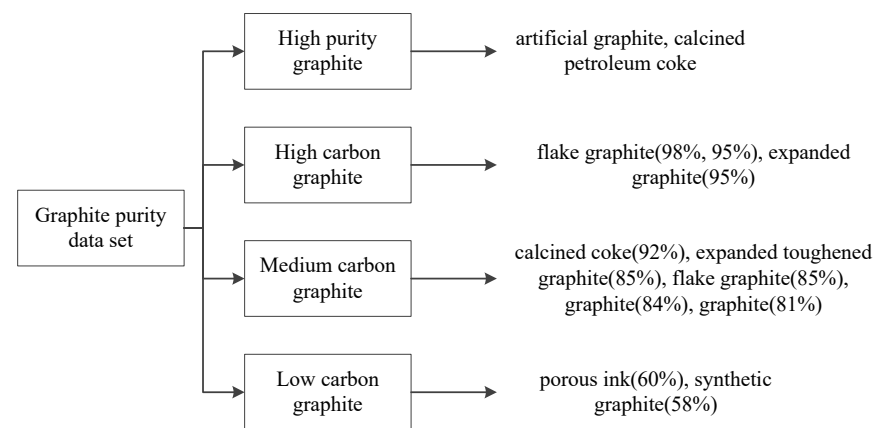


Figure 2. Graphite purity data set.

The sample images and videos are taken from different angles at the same position at noon by using the rear camera of an iPhone, and the resolution of the video is 1080p; the captured graphite video was extracted by frame, 1 frame per second. After screening, 306 sample images are obtained and classified. During the experiment, all the images are obtained from the saved data. Four types of graphite with different purity are shown in Figure 3.

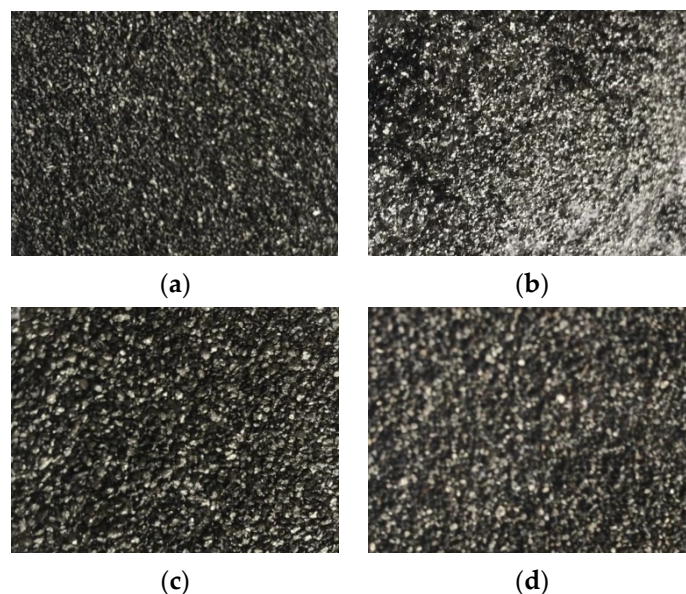


Figure 3. Four types of graphite with different purity. (a) High-purity graphite; (b) High-carbon graphite; (c) Medium-carbon graphite; (d) Low-carbon graphite.

2.2. Data Augmentation

In order to reduce the imbalance of samples and solve the problem of overfitting, easily caused by too-small data sets, another training data set is generated by data expansion technology based on the initial data set. In order to improve the efficiency of image processing, the graphite image is cut out from the image. The original size is 1080 pixels, and the smaller image is 396 pixels. To solve the problem of insufficient training samples, this paper expands the data set obtained offline. The data enhancement stage reveals several different expression modes of the original image. The collected images are enhanced by different enhancement technologies, such as brightness enhancement, contrast enhancement, horizontal rotation and random square rotation, which have different degrees of pixel brightness. Finally, 1530 images were obtained.

Of these, 1224 samples (80%) were randomly selected as the training data set to train the network, and 306 samples (20%) were selected as the testing data set to verify the performance of the network. The training set and the test set were processed separately.

The classification of data sets is shown in Table 1.

Table 1. Graphite data set.

	High-Purity Graphite	High-Carbon Graphite	Medium-Carbon Graphite	Low-Carbon Graphite
Data set	315	395	530	290
Training set	252	316	424	232
Test set	63	79	106	58

Based on the characteristics of the graphite image, the training set images are randomly scrambled before input to reduce the influence of image order on the model; at the same time, in the process of training, the image of the data set is enhanced online. Each image in the training set is cut randomly, and the image pixels are unified. The image is flipped horizontally according to the probability (set $p = 0.5$). Finally, the processed data set is normalized, and the data of each channel are regularized with the mean value 0.5 and the standard deviation 0.5. After the data set is processed in this way, the image is entered into model training (shown in Figure 4).

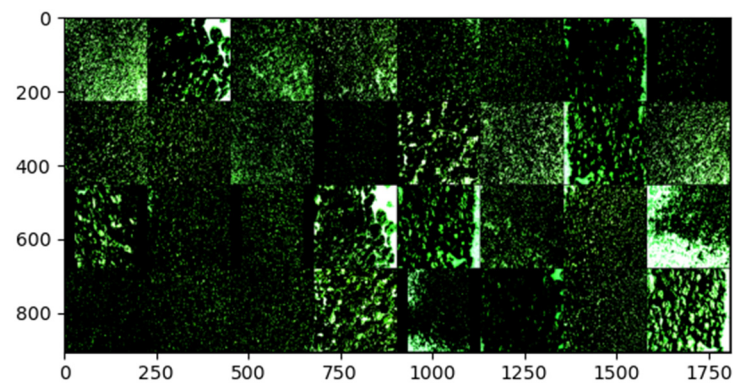


Figure 4. Image of a batch after data enhancement.

3. Experimental Principle and Method

3.1. Transfer Learning

In recent years, deep CNN has been the mainstream method to solve challenging computer vision tasks. However, training a network from scratch requires a lot of training data, time and a Graphics Processing Unit (GPU). The number of parameters in a CNN model increases with the increase in the network. The deeper the network is, the more complex the calculation—and the higher the requirement of training data. In this paper, there are only 1530 training and test images, and a small data set cannot train a deep CNN. Therefore, this paper combines the idea of transfer learning to train CNN.

Transfer learning refers to the process of using models that have been trained for different tasks, hoping that the model can have enough generalized information to solve new specific tasks [12]. Transfer learning uses a huge database of pre-training models (CNN models) to help learn target tasks [13–16]. In the application of this transfer learning technology, large image data mostly belong to the general images field, such as those of a cat, dog or chair. The image in this paper is graphite, which has a different visual performance. The visual performance learned from these large images may not be able to represent graphite images well. Therefore, we need to modify the pre-trained CNN structure to adapt to our task. Donahue, Zeiler and Fergus provide evidence that the general image representation learned from the pre-trained CNN is superior to the most advanced hand-made features [17,18].

AlexNet, VGG16, Residual Net 34 (ResNet34) and Mobile Net Vision 2 (MobileNet V2) are all popular pre-trained CNNs. These networks are good for researchers because they require shorter training time, weaker and cheaper hardware requirements and reduce the amount of calculation.

3.2. Multi-Model Weighted Feature Fusion Mechanism

In deep learning, the extracted features contain local and global information, and the significant advantage of deep learning is to verify the system with the best accuracy on large data sets [19]. In this paper, the shallow AlexNet network and the deep ResNet50 network are selected as the basic models to extract the global and local features of the graphite data set, respectively.

(1) AlexNet network

The AlexNet network consists of eight layers, including five layers of convolution layer (conv) and three layers of full connection layer (FC). There are also three pools in the AlexNet network. Moreover, the convolution layer and pooling layer are connected alternately. The structure of the AlexNet network is shown in Figure 5. Compared with other existing networks, such as Visual Geometry Group (VGG), GoogLeNet, Mobile Net and so on, AlexNet has a simpler network structure and fewer network parameters, so it is not very difficult to train and has strong representation ability [20]. Based on the above advantages, this paper selects the AlexNet network as one of the feature-extraction

networks of graphite precision images and focuses on extracting the overall features of graphite data sets.

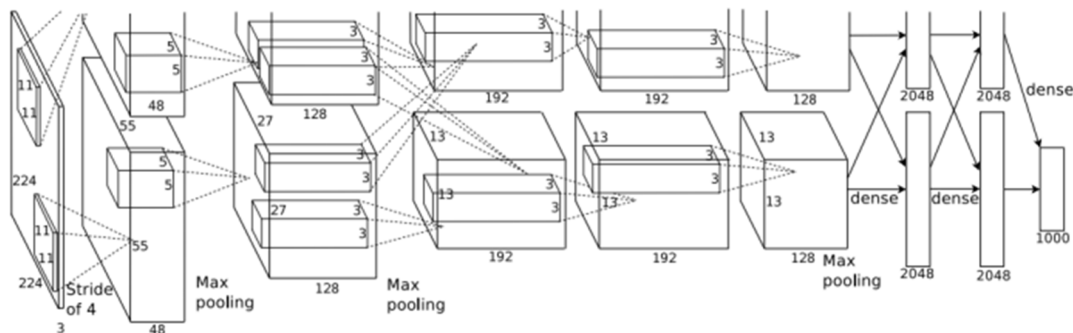


Figure 5. AlexNet network structure.

(2) ResNet50 network

ResNet is one of the models developed by He et al. in 2016. The formation of this architecture is to overcome the difficulties in deep-learning training, because deep-learning training usually takes a lot of time and is limited to a certain number of layers [21]. Compared with other architecture models, the advantage of the ResNet model is that even if the architecture is deeper and deeper, its performance will not be reduced. The ResNet model protects the integrity of information by transmitting the input information directly to the output [22]. The whole network only needs to learn the difference between input and output, which simplifies the learning goal and difficulty [23].

ResNet34, ResNet50, ResNet101 and ResNet152 are typical frameworks of ResNet. In this paper, ResNet50 is selected as the bottom-up feature-extraction path for several reasons: because the experiment in Reference [24] shows that ResNet50 has a lower error rate than ResNet18 and ResNet34; the number of parameters required is half that of ResNet101 and ResNet152; and the self-built graphite precision data set in this paper is small, so the ResNet50 model can be used to extract image features well.

(3) Feature fusion

Feature fusion extracts different types of features from images by a variety of feature-extraction methods, fuses the features according to specific methods, and finally forms a new feature vector. Feature fusion can retain a variety of highly representative features, thus preserving the useful information of the image as much as possible [24].

In this paper, the feature fusion algorithm based on deep-learning theory combines the features obtained by optimized AlexNet and ResNet50.

The feature fusion methods can be series, parallel and weighted average [24]. For the images in graphite data sets, this paper uses the weighted fusion method to directly series the two feature vectors to form the fused feature vector, which is used as the final feature of graphite precision recognition. This enables the network to selectively enlarge valuable and meaningful feature channels based on global information and suppress relatively useless feature channels, so as to continuously improve the representation ability of deep features [25]. For images in a graphite data set, the different sizes of the two feature vectors may have different feature point ratios. For that reason, this paper uses the weighted fusion method to connect the two feature vectors directly in series, to generate a new feature vector as the final feature of graphite precision recognition. The fusion mechanism of this paper is shown in Figure 6.

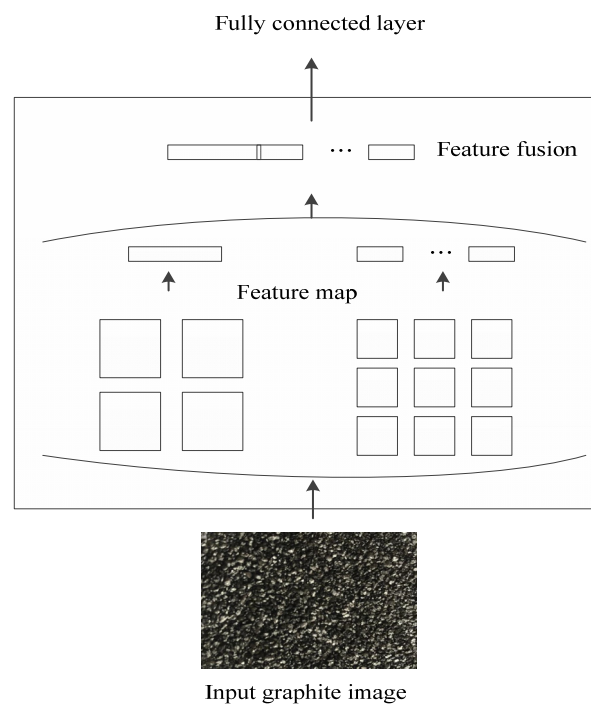


Figure 6. The fusion mechanism of this paper.

3.3. Experimental Methods

Combined with transfer learning, this paper implements dual-channel feature extraction on a graphite precision data set and loads the weights of AlexNet and AlexNet50 at the same time. Because there are many parameters in the full connection layer of AlexNet, it is easy to overfit, so this paper redesigns the full connection layer of AlexNet.

In the AlexNet network, the linear activation of Rectified Linear Units (ReLU) in the region of the network may cause the value after activation to be too large and affect the stability of the model. This will reduce the training speed of the network, and may even reduce the generalization performance of the network. To counteract the linear growth of ReLU, we use the ReLU6 function, and its graphics are shown in Figure 7. In low-precision calculations, the dynamic range can be compressed, the convergence speed is faster and the utilization rate of parameters is increased, which makes the algorithm more robust.

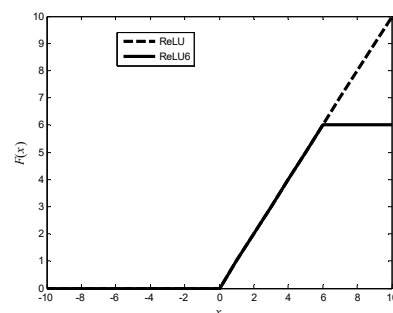


Figure 7. Graphs of ReLU6 and ReLU.

In the full connection layer, dropout is used to randomly ignore some neurons, which can effectively solve the overfitting problem and improve the overall robustness of the model. Finally, the final classification layer of Softmax nonlinear is used, and the final output is set to 4. The optimized AlexNet output module is shown in Figure 8.

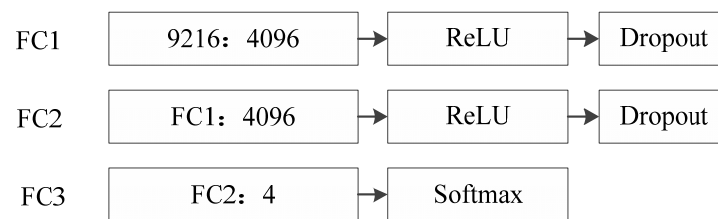


Figure 8. Optimized AlexNet full connection layer.

The dual-channel feature-extraction process designed in this paper is shown in Figure 9, and the weight ratio of optimized AlexNet and ResNet50 is set to 3:7.

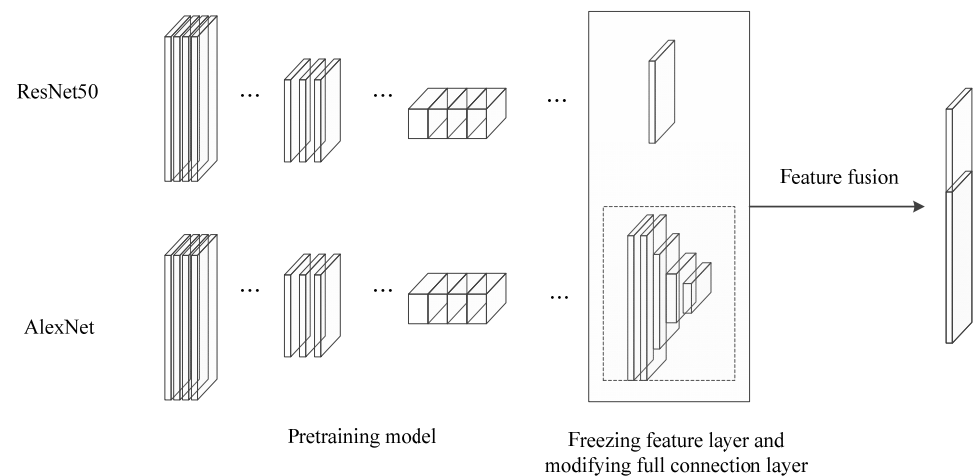


Figure 9. Dual-channel feature-extraction process.

In order to fine-tune the network, an Adam optimizer performs 50 epoch iterations for all models, with 0.0001 as the initial learning rate and Nesterov momentum set to 0.9. Under the conditions of this model, cross entropy is still used as the loss function, and the super parameters are adjusted on the testing data set.

In summary, the specific calculation flow of the whole network structure is shown in Figure 10. In this paper, this model is called convolution neural network model combined with transfer learning and multi-model weighted fusion mechanism, which is applied to graphite purity classification.

Combined with transfer learning, a graphite purity recognition method based on a multi-model weighted fusion mechanism is proposed in this paper. The self-built graphite purity small sample data set is expanded offline and enhanced online to enhance the generalization ability of the model. In the multi-pool convolution operation, multi-layer features may lose the depth, shape and the relationship information between the target and the scene, which limits recognition accuracy. In order to solve this problem, this paper designs the optimized AlexNet network and ResNet50 network, designs the dual-channel convolution network model, weights and fuses the extracted features, extracts the deep-seated features of the graphite image, and enhances the stability of the overall model and the accuracy of recognition.

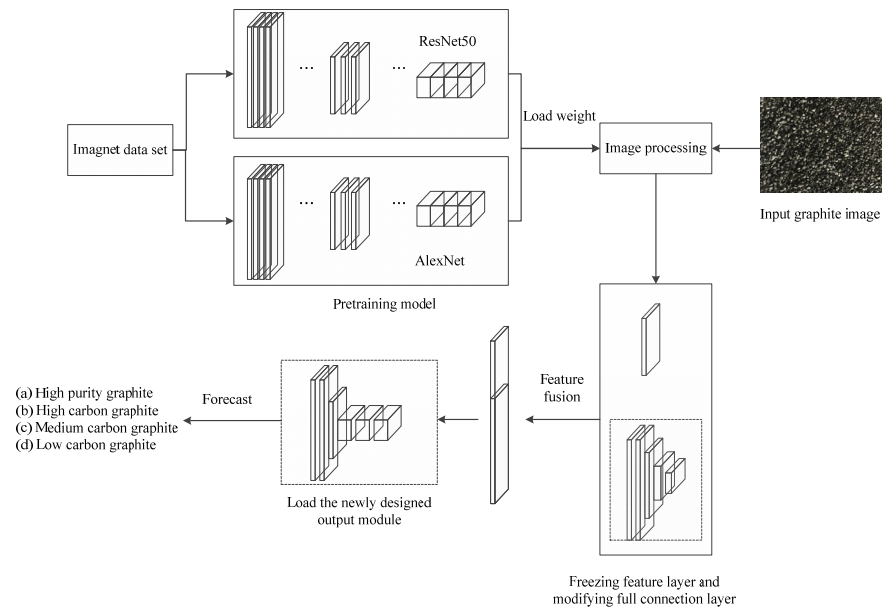


Figure 10. Convolution neural network model with multi-model weighted fusion mechanism combined with transfer learning.

4. Experiments

4.1. Evaluation Index and Environmental Allocation

In this paper, the training effect of a network is evaluated by accuracy (ACC), loss and running time. Test ACC refers to the ratio of the model output correct results in the test set, which can reflect the use effect of a network and is a very important index. The definition formula is shown in Equation (1):

$$acc = \frac{n_{correct}}{n} \quad (1)$$

where, $n_{correct}$ is the number of correct network identifications in the test set, and n is the number of samples in the test set.

The training process of transfer learning is to minimize the loss function, and loss is the value of the loss function. In fact, the loss function calculates the mean square error (MSE) of the model on the test set, as shown in Equation (2):

$$E = \frac{1}{n} \sum_i (y^{test} - \hat{y}^{test})^2 \quad (2)$$

In this paper, the epoch time is specified by the end of the whole network model. An epoch is a process in which all training samples are propagated forward and backward in the neural network model, that is, all training samples are trained once.

In this paper, we use the 1.8.0 version of Python framework to complete the experimental simulation under the compiling environment of Python 3.8, and realize the image data preprocessing through transform. The experimental environment is the Windows 10 operating system, and the processor is Intel (R) core (TM) i9-10900f CPU.

4.2. Experimental Result

(1) Batch size setting

In order to make the parameters of the algorithm relatively optimal, this paper analyzes different batch_sizes, and the results are shown in Figure 11. When the batch_size is 16, the accuracy fluctuates greatly and the robustness of the whole model is not strong, when the batch_size is 32 and 64, the accuracy fluctuates less and improves faster, and when the batch_size is 32, the model converges quickly. At the same time, considering the accuracy and convergence rate, this paper finally selects the batch_size as 32.

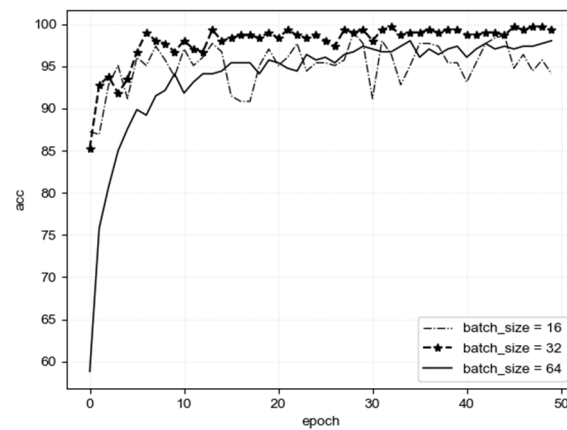


Figure 11. Comparison of experimental results of training networks with different batch_sizes.

(2) Network optimization

In this paper, training is based on AlexNet and ResNet50 networks. In order to improve the stability of AlexNet, the output module of AlexNet is redesigned and loaded into the full connection layer. The comparison results are shown in Figure 12.

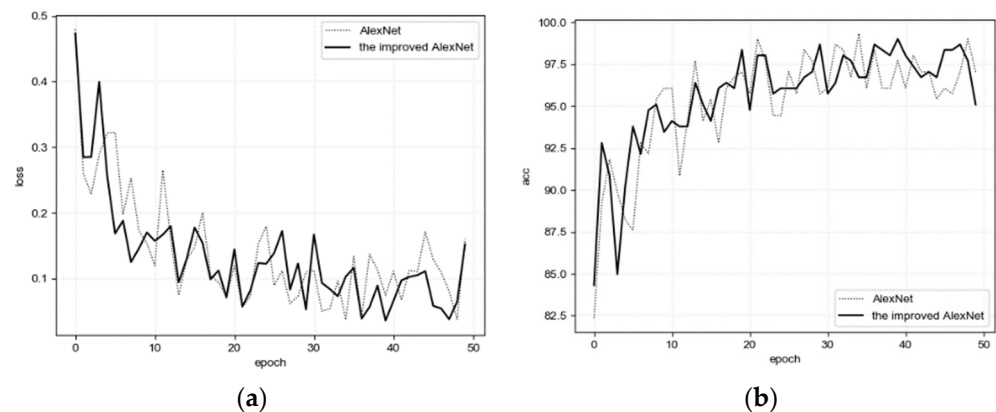


Figure 12. Comparison results of AlexNet and optimized AlexNet. (a) loss; (b) acc.

It can be seen from Figure 12 that the optimized AlexNet makes the network more stable. After modifying the activation function, with the increase in epoch, the loss value decreases rapidly, and the accuracy rate improves slightly, which verifies the effectiveness and feasibility of the optimized AlexNet. The comparative loss and accuracy rate are shown in Table 2.

Table 2. Loss and accuracy of AlexNet and optimized AlexNet.

Method	Loss ($\times 10^{-2}$)	Acc (%)
AlexNet	3.76	93.29
Optimized AlexNet	3.60	95.67

(3) Comparative analysis of network structure

In order to verify the role of optimized AlexNet and ResNet50 in graphite purity feature representation, experiments were carried out to give different weights to the data set, and the accuracy of graphite recognition was recorded. The results are shown in Figure 13. It can be seen that when the weight ratio of the features extracted by AlexNet and ResNet50 is 3:7, the recognition accuracy fluctuates little, and the accuracy is relatively optimal, so the final weight ratio is 3:7.

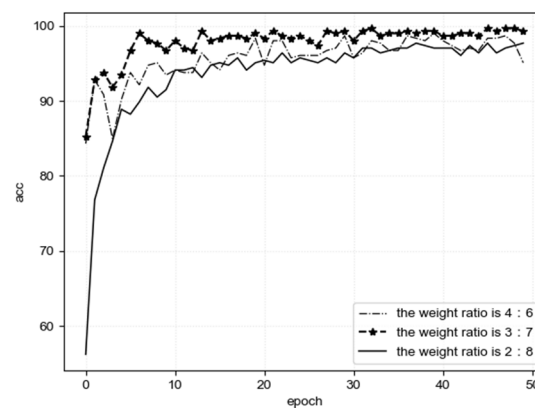


Figure 13. Model accuracy under different weight ratios.

In order to verify the feasibility of the proposed multi-model weighted fusion mechanism to extract graphite image features, the control groups are AlexNet, optimized AlexNet, ResNet50 and AlexNet + ResNet50, which are compared with the optimized AlexNet + ResNet50. The graphite data set after data enhancement is imported into the method proposed in this paper. The experimental results of the test set are shown in Figure 14.

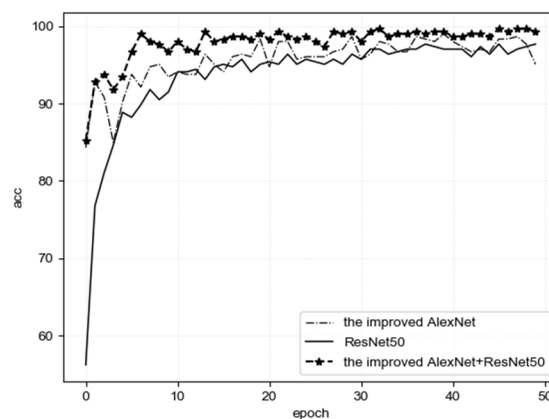


Figure 14. Accuracy comparison curves of different algorithms.

As can be seen from Figure 14, the multi-model feature weighted fusion algorithm proposed in this paper increases the convergence speed of the model, while its accuracy rate gradually increases and tends to be stable with the increase in epoch times. The accuracy rate of the algorithm in this paper is relatively optimal, which indicates that the algorithm can effectively improve the stability and robustness of the overall model. The comparison between accuracy rate and model training time is shown in Table 3, which further verifies the effectiveness of the proposed algorithm.

Table 3. Accuracy comparison of different algorithm models.

Method	Acc (%)	Training Time (min)
AlexNet	93.29	89.69
Optimized AlexNet	95.67	95.01
ResNet50	94.05	99.75
AlexNet + ResNet50	96.69	142.70
Optimized AlexNet + ResNet50	97.94	120.92

5. Conclusions

In this paper, a graphite purity identification method based on a multi-model weighted fusion mechanism combined with transfer learning is proposed. The offline expansion

and online enhancement of the self-built graphite purity small sample data set enhance the generalization ability of the model. The optimized AlexNet and ResNet50 are used to construct a dual-channel convolution neural network, and the features extracted by the two are weighted and fused to enhance the stability of the overall model and the accuracy of recognition. Experimental results show that the recognition accuracy of graphite based on the multi-model feature fusion mechanism is better than that of a single-feature mechanism of AlexNet or ResNet50. Recognition accuracy reaches 97.94%, which is of great significance to the development of the graphite field. Although the algorithm in this paper has achieved good results in graphite purity identification, it still needs a long time to train the overall model. In future work, we will focus on reducing the training time of the model and applying it to large data sets.

Author Contributions: Conceptualization, X.X. and X.Y.; methodology, F.W.; software, X.X.; validation, X.X., X.Y. and F.W.; formal analysis, G.L.; investigation, G.L.; resources, X.X.; data curation, G.L.; writing—original draft preparation, X.X.; writing—review and editing, X.Y.; visualization, G.L.; supervision, X.X.; project administration, G.L.; funding acquisition, X.X. All authors have read and agreed to the published version of the manuscript.

Funding: This research received no external funding.

Institutional Review Board Statement: Not applicable.

Informed Consent Statement: Not applicable.

Data Availability Statement: The data sets used and/or analyzed during the current study are available from the corresponding author on reasonable request.

Acknowledgments: This work is supported by the Innovation Capability Support Program of Shaanxi Province of China (Grants No. 2020PT-023), National Natural Science Foundation of China (Grants No. 11801438) and Natural Science Basic Research Plan in Shaanxi Province of China (Grants No. 2018JQ1089).

Conflicts of Interest: The authors declare no conflict of interest.

References

1. Liu, M.Q.; Jiao, Y.Y.; Qin, J.C.; Li, Z.; Wang, J. Boron doped C_3N_4 nanodots/nonmetal element (S, P, F, Br) doped C_3N_4 nanosheets heterojunction with synergistic effect to boost the photocatalytic hydrogen production performance. *Appl. Surf. Sci.* **2021**, *541*, 148558. [[CrossRef](#)]
2. Zhang, X.D.; Qiu, Y.L.; Wu, Y.M.; Wang, S.J.; Zhang, L.Y. Effect of raw material characteristics and preparation process on thermal conductivity of flexible graphite film. *Silic. Bull.* **2019**, *38*, 3988–3992.
3. Rao, J.; Zhang, P.; He, S.; Li, Z.H.; Ma, H.W.; Shen, Z.P.; Miao, S.D. Utilization status of natural graphite and review of graphite products. *Chin. Sci. Technol. Sci.* **2017**, *47*, 13–31.
4. Jalili, M.; Ghanbari, H.; Bellash, S.M.; Malekfar, R. High-quality liquid phase-pulsed laser ablation graphene synthesis by flexible graphite exfoliation. *J. Mater. Sci. Technol.* **2019**, *35*, 292–299. [[CrossRef](#)]
5. Li, Y.; Zhang, S.Y. Status and prospect of high purity graphite production process. *Sci. Technol. Innov.* **2018**, *1*, 166–167.
6. Wu, B.; Yuan, S.; Li, P.; Jing, Z.; Huang, S.; Zhao, Y. Radar emitter signal recognition based on one-dimensional convolutional neural network with attention mechanism. *Sensors* **2020**, *20*, 6350. [[CrossRef](#)]
7. Rashid, M.; Khan, M.A.; Alhaisoni, M.; Wang, S.-H.; Naqvi, S.R.; Rehman, A.; Saba, T. A sustainable deep learning framework for object recognition using multi-layers deep features fusion and selection. *Sustainability* **2020**, *12*, 5037. [[CrossRef](#)]
8. Li, X.L.; Niu, H.T. Facial expression recognition based on feature fusion of VGG-NET. *Comput. Eng. Sci.* **2020**, *42*, 500–509.
9. Brahim, M.; Boukhifa, K.; Moussaoui, A. Deep learning for tomato dis-eases: Classification and symptoms visualization. *Appl. Artif. Intell.* **2017**, *31*, 1–17. [[CrossRef](#)]
10. Khan, A.; Chefranov, A.; Demirel, H. Image scene geometry recognition using low-level features fusion at multi-layer deep CNN. *Neurocomputing* **2021**, *440*, 111–126. [[CrossRef](#)]
11. Chen, Y.R.; Tian, Q.H.; Yang, H.M.; Liang, Q.L.; Bao, J.X. Static gesture recognition based on multi-feature weighted fusion. *Comput. Syst. Appl.* **2021**, *30*, 20–27.
12. Lu, J.; Behbood, V.; Hao, P.; Zuo, H.; Xue, S.; Zhang, G. Transfer learning using computational intelligence: A survey. *Knowl.-Based Syst.* **2015**, *80*, 14–23. [[CrossRef](#)]
13. Yin, L.; Wang, L.; Huang, W.; Liu, S.; Yang, B.; Zheng, W. Spatiotemporal Analysis of Haze in Beijing Based on the Multi-Convolution Model. *Atmosphere* **2021**, *12*, 1408. [[CrossRef](#)]

14. Zhang, X.; Tang, Y.; Zhang, F.; Lee, C.-S. A Novel Aluminum-Graphite Dual-Ion Battery. *Adv. Energy Mater.* **2016**, *6*, 1502588. [[CrossRef](#)]
15. Zhang, Z.; Tian, J.; Huang, W.; Yin, L.; Zheng, W.; Liu, S. A Haze Prediction Method Based on One-Dimensional Convolutional Neural Network. *Atmosphere* **2021**, *12*, 1327. [[CrossRef](#)]
16. Tajbakhsh, N.; Shin, J.Y.; Gurudu, S.R.; Hurst, R.T.; Kendall, C.B.; Gotway, M.B.; Liang, J. Convolutional neural networks for medical image analysis: Full training or fine tuning? *IEEE Trans-Actions Med. Imaging* **2016**, *35*, 1299–1312. [[CrossRef](#)]
17. Rahim, T.; Hassan, S.A.; Shin, S.Y. A deep convolutional neural network for the detection of polyps in colonoscopy images. *Biomed. Signal Processing Control.* **2021**, *68*, 1–21. [[CrossRef](#)]
18. Zeiler, M.D.; Fergus, R. Visualizing and understanding convolutional networks. In *European Conference on Computer Vision*; Springer: Cham, Switzerland, 2014; pp. 818–833.
19. Saeed, F.; Khan, M.A.; Sharif, M.; Mittal, M.; Goyal, L.M.; Roy, S. Deep neural network features fusion and selection based on PLS regression with an application for crops diseases classification. *Appl. Soft Comput.* **2021**, *103*, 107164. [[CrossRef](#)]
20. Gan, L.; Guo, Z.H.; Wang, Y. Image recognition method of gastric tumor cells based on radial transform and improved AlexNet. *Comput. Appl.* **2019**, *39*, 2923–2929.
21. He, K.M.; Zhang, X.Y.; Ren, S.Q.; Sun, J. Deep residual learning for image recognition. In Proceedings of the 2016 IEEE Conference on Computer Vision and Pattern Recognition, Las Vegas, NV, USA, 27–30 June 2016; pp. 770–778.
22. Devvi, S.; Hilya, P.R.; Alhadi, B.; Pinkie, A. Deep learning in image classification using Residual Network (ResNet) variants for detection of colorectal cancer. *Procedia Comput. Sci.* **2021**, *179*, 323–431.
23. Chen, J.Y.; Yang, T.J.; Zhang, D.M.; Huang, H.; Tian, Y. Deep learning based classification of rock structure of tunnel face. *Geosci. Front.* **2021**, *12*, 395–404. [[CrossRef](#)]
24. Zhang, W.C.; Chen, L.H.; Wu, W.; Yang, X.M.; Yan, B.Y. Traffic sign recognition based on convolutional neural network feature fusion. *Comput. Appl.* **2019**, *39*, 21–25.
25. Zhang, R.; Zhuo, L.; Zhang, H.; Zhang, Y.; Kim, J.; Yin, H.; Zhao, P.; Wang, Z. Vestibule segmentation from CT images with integration of multiple deep feature fusion strategies. *Comput. Med. Imaging Graph.* **2021**, *89*, 101872. [[CrossRef](#)] [[PubMed](#)]